HUGHES

RESEARCH LABORATORIES

INVESTIGATION OF R-F NOISE GENERATION FROM SPACE VEHICLES

Quarterly Report No. 1
Contract NAS 8-862

24 June 1961 through 24 October 1961

HUGHES RESEARCH LABORATORIES
Malibu, California

a division of hughes aircraft company

INVESTIGATION OF R-F NOISE GENERATION FROM SPACE VEHICLES

Quarterly Report No. 1
Contract NAS 8-862

24 June 1961 through 24 October 1961

TABLE OF CONTENTS

LIST OF ILLUSTRATIONS

I. INTRODUCTION

This report describes the work on r-f noise generation from the electrical propulsion engine and plasma beams of space vehicles which was carried out by the Hughes Research Laboratories during the period 24 June 1961 through 24 October 1961. The results of the work done under NASA Contract NAS 8-862 are discussed.

The primary objective of this program is to determine the r-f noise generated by typical plasma propulsion engines. In addition, the effects of such r-f noise on communication with space vehicles is to be evaluated. The program should yield information and criteria pertinent to the design of low-noise communication channels. The importance of the program is connected with the necessity of maintaining reliable communications with personnel or equipment on board a space vehicle.

During this initial report period, the scope and main aspects of the program were detailed. The types of noise expected were tabulated, and it was found that a noise growth mechanism may possibly occur. Directional effects on the noise radiation were listed. Operating parameters of the plasma engine which affect the r-f noise were determined, and suitable typical values of these parameters were selected for quantitative noise calculations. Models of the plasma wake and the space vehicle receiving antennas were considered and are proposed in this report.

One of the main purposes of this initial analytical effort was to obtain information to help guide the course of the future experimental program. Therefore, plans for experiments were deferred until the analytical information was available. During the past quarter, several sources of r-f noise were investigated analytically; some results obtained are presented here.

II. OUTLINE OF PROGRAM

A. TYPES OF NOISE

R-f noise generated by plasma engines may be subdivided into two main categories: (a) noise common to all plasma engines, and (b) noise occurring only in particular types of engines.

1. Noise Mechanisms Common to All Plasma Engines

a. Electron-ion collisional radiation -- This is often referred to as bremsstrahlung. It is expected that this will be one of the dominant radiation mechanisms.

b. Radiation from elastic collisions with neutral atoms — Both electrons and ions can collide elastically with neutral atoms. The neutral atoms constitute the background in space (or other engine environment), or are ejected from the plasma engine as nonionized particles.

c. Acceleration radiation — Either ions or electrons or both are accelerated from thermal velocities to exhaust velocities by the plasma engine.

d. Potential variation radiation — Electrons or ions radiate due to acceleration in potential variations in the plasma. These variations are macroscopic and may arise as follows:

(1) Plasma boundaries — An electron sheath is set up at the edge of the plasma, which results in a potential well across the plasma. This appears to be one of the dominant noise mechanisms.

(2) Electrostatic collective oscillations — Such as plasma oscillations, plasma boundary ripples.

(3) Mechanical collective oscillations — Such as acoustical waves set up by mechanical vibrations.

(4) Traps — These result as a combination of electrode and particle potentials and arise from different causes in the various plasma engines.

e. Recombination radiation — This is largely confined to optical frequencies and probably does not interfere with frequencies suitable for communications.

f. Excitation radiation — This is largely confined to optical frequencies.

g. Charge exchange radiation — This is possibly a substantial noise mechanism in the r-f range.

h. Cathode shot noise — This arises from random emission of electrons or ions from cathodes. The electron cathode shot noise occurs in all plasma engines, whereas the ion cathode emission may be absent in some plasma engines (Penning engine, for example).

i. Cathode flicker noise -- This depends on frequency as the inverse square and should be negligible beyond audio frequencies.[1]

j. Black body radiation — This arises from hot electrodes or surfaces internal to the plasma engine.

2. Noise Mechanisms in Particular Plasma Engines

The plasma engines considered in this contract are the (cesium) electrostatic ion engine, the Penning engine, and the r-f engine.

a. Ion engine — This has no sources of radiation other than those already mentioned. In this engine, trapping is caused by strong potential wells created by the ion beam before neutralization and by potential wells set up by the electrode system.

b. Penning engine — The internal magnetic field of this engine gives rise to an additional radiation mechanism — cyclotron radiation. Trapping in this engine occurs as a result of magnetic mirror action in the inhomogeneous magnetic field. Because the magnetic fields are generally small, of a few tens of gauss, both noise mechanisms are expected to be negligible.

c. R-f engine — In this engine, r-f fields are used to accelerate a plasma. There may be leakage radiation from the power source and from the r-f circuit. Also, r-f modulation of velocities or densities in the plasma may lead to additional radiation. Power at this frequency is largely coherent and does not constitute noise as such. However, communications systems must discriminate against this frequency. Trapping can occur if the r-f wave is synchronous or quasi-synchronous with the plasma motion. Ions tend to concentrate in bunches, along the wave troughs, and so create potential wells.

3. Unimportant Noise Mechanisms

Other noise mechanisms exist which are unimportant for various reasons. These are listed for completeness.

a. Black-body radiation from plasma -- The plasma ejected from plasma engines generally is neither optically thick nor in thermal equilibrium. Hence it does not obey the black-body-radiation laws. The various collisional processes considered replace the black-body radiation.

b. Cyclotron radiation in space — Magnetic fields in space are of order 10^{-4} to 10^{-5} gauss. Such fields give rise to negligible radiation, inasmuch as a typical cyclotron radius is much larger than typical plasma beam thicknesses.

c. Cerenkov radiation — Fast electrons moving through a plasma can give rise to Cerenkov radiation. The required velocities are so large that only a very few electrons can contribute any radiation.

d. Alfven waves — Magnetic fields in space are so small that no appreciable Alfven waves occur. Such waves would set up potential variations in the plasma, which would lead to radiation.

e. Plasma oscillations — These are longitudinal, body, oscillations, which do not radiate any energy. However, magnetic fields, density fluctuations, and other mechanisms may couple the plasma oscillations to transverse waves, which can radiate energy.

B. NOISE GROWTH MECHANISM

The plasma beam ejected from most plasma engines consists of essentially monoenergetic ions and of electrons with a spread of velocities but presumably having the same axial drift velocity as the ions. A double stream instability may develop, the exact nature of which depends rather critically on the precise form of the electron velocity distribution. This velocity distribution is not at all well known in present plasma engines. Conditions near the exhaust plane apparently favor the onset of this instability, whereas conditions far downstream along the plasma beam are apparently unfavorable for the instability.

If the plasma beam has a definite end from which electrons or ions can be reflected, then multistreaming of particles occurs, and it is likely that the double stream instability sets in.

The instability may amplify broad-band noise by a small amount, as well as amplifying a narrow frequency range (and its harmonics) by a large amount.

C. DIRECTIONAL EFFECTS ON RADIATION

1. Directional Emission of Radiation

The collisional radiation is a dipole-type radiation. Acceleration radiation, resulting from plasma engine potentials, is also dipole radiation with a well-defined direction. Radiation by acceleration in electrostatic potential wells or magnetic mirrors is also essentially dipole radiation. Since the ions normally have a well-defined direction, radiation from them is strongly polarized. Electrons usually have thermal velocities which are large compared with their directed velocities and should radiate isotropically.

2. Collimation of Internal Radiation

Radiation emitted inside the plasma engine is collimated in escaping outside. Such radiation is strongly directed into the plasma beam and away from the space vehicle. This directivity is modified by the fields induced upon, and reradiated from, the electrodes.

3. Directional Effects of the Plasma Beam

a. Dielectric focusing — The plasma acts as a negative dielectric to certain frequencies. The variation of electron density in the plasma beam causes focusing of these frequencies. For the conical plasma beam model, low frequencies are strongly focused directly away from the space vehicle.

b. Selective attenuation — Some frequencies can propagate freely through the plasma. Waves of these frequencies are attenuated in propagating through the plasma. Usually the plasma is much longer than it is thick; therefore, more radiation escapes in the radial direction than along the plasma beam axis.

4. Noise Source Extent and Location

The extent and location of the noise source together with the pattern and axial direction of a receiving antenna affect the fraction of the total noise that can be detected by that antenna. As the plasma beam resembles a line source of radiation, this results in a large reduction in actual antenna noise for a particular model considered.

D. NOISE PARAMETERS

1. Important Parameters

a. Density of all particle types.

b. Velocity, directed and thermal, of all particle types.

c. Temperature of all hot, solid surfaces in plasma engine.

d. Potential variation in acceleration regions of plasma engine.

e. Dimensions and shape of plasma beam.

f. Types of particles.

g. Receiving antenna radius.

2. Typical Parameter Values

Reasonable estimates of most of the parameters can be made for all types of plasma engines. The parameters below correspond to possible values for the cesium ion electrostatic engine. These parameters generally result in maximum values of noise radiation and are the values used in quantitative noise estimates. Hence, the noise powers quoted are usually overestimated.

a. Electron or ion density: $10^{16}/m^3$ at engine exhaust plane.[2]
Atom density in space: $10^6/m^3$.[3]
Nonionized neutral atom density from engine: $2.7 \times 10^{17}/m^3$ at engine exhaust plane.

b. Electron or ion directed velocity: 1.20×10^5 meters/sec (corresponding to 10 kv cesium ions).
Ions and nonionized neutral atoms, thermal velocity: 4.82×10^2 meters/sec (corresponding to 1200° K cesium ions, atoms).
Electron thermal velocity: 1.325×10^6 meters/sec (corresponding to 5 volts).

c. Hot surfaces in ion engine are electrodes at 1200° K.

d. Ion potential differences of 20 kv and 10 kv with field strengths of 1.325 Mv/meter and 2.86 Mv/meter acceleration and deceleration regions (ion engine).

e. At engine exhaust plane, plasma with annular shape 0.001 meter thick and 0.075 meter mean diameter. A cluster of 22 engines is assumed; thus the total ion current is 10 amperes. If an equivalent cylindrical plasma is used for the engine cluster, its initial radius is 0.129 meter.

f. Cesium ions and neutral atoms from engine.
Hydrogen atoms in space.[3]

g. Receiving antenna radius: 1 meter.

III. MODELS

A. PLASMA WAKE MODELS

Models are proposed for the charged particle density variation in the plasma. The charged particle density has important effects on noise generated in the plasma, as well as on the noise growth mechanism and plasma directive effects.

Thermal effects, instabilities, and microscopic lack of neutralization all cause expansion of the plasma and a resultant density variation. Because of its over-all neutrality, there is no macroscopic space-charge spreading of the plasma.

Only thermal expansion is considered here. The mean free path (in the background space gas) of plasma particles is appreciably larger than the initial plasma thickness. Under these conditions, thermal expansion is caused by free expansion rather than by diffusion into the space gas.

The axial velocity (z velocity) of the charged plasma particles is given by the drift velocity of the ions at the engine exhaust plane. If the plasma expands at constant radial velocity and has uniform density over any cross section, then the proper model of the plasma is a (truncated) cone. This model is now justified.

Consider first the radial velocity with which the plasma expands. It is sufficient to consider the expansion of a long cylinder of plasma. Let the cylinder have initial radius r. The ions of mass M all have the same radial velocity v, and the electrons of mass m all have a radial velocity v'. Ignore collisions. Then, at a long time t later, the plasma is uniformly dense in an annular cylinder of thickness $2r$ and mean radius $v_o t$, where

$$v_o = \frac{M}{M+m} v + \frac{m}{M+m} v' \approx v + \frac{m}{M} v' \quad .$$

This follows from conservation of momentum and simple geometrical considerations. Ordinarily,

$$v >> \frac{mv'}{M}$$

so that

$$v_o \approx v \quad .$$

The plasma expands with nearly the ion radial velocity.

Collisions do not significant affect the results provided that v is only slightly changed in a distance r.

Now consider a Maxwellian distribution of ion radial velocities. The normalized density of particles at a radius R, after expansion, is nearly given by[4]

$$n(R,t) = \left(\frac{M}{\pi kT}\right)^{1/2} \frac{e^{-MR^2/2kTt^2}}{2\pi Rt} \;, \qquad \begin{array}{l} R \gg r \\[2ex] t \gg r \left(\frac{M}{2kT}\right)^{1/2} \end{array} \quad .$$

Here, k is Boltzmann's constant and T is the temperature. Observe that $v_T = \left(\frac{2kT}{\pi kT}\right)^{1/2}$ is the transverse part of the ion rms thermal velocity. The normalized number of particles in an incremental area of the cross section is

$$n(R,t)\, Rdrd\theta = \left(\frac{M}{\pi kT}\right)^{1/2} \frac{e^{-MR^2/2kTt^2}}{2\pi t} \, dRd\theta \quad .$$

Essentially, this is independent of R out to $R = v_T t$ and zero thereafter.

These considerations justify a model for the plasma in which the radius grows linearly with time as $v_T t$ and which has a uniform particle density (in Cartesian coordinates, where metric coefficients do not obscure the behavior or notation) over its entire cross section.

The situation for the growth of an initial cylindrical plasma is illustrated in Fig. 1. The ions have an axial velocity of $v_o \gg T$. If n_o is the initial density at the exhaust plane, z = 0, then the density n(z) is

$$n(z) = n_o \frac{1}{\left(1 + \frac{vTz}{v_o R}\right)^2} \quad .$$

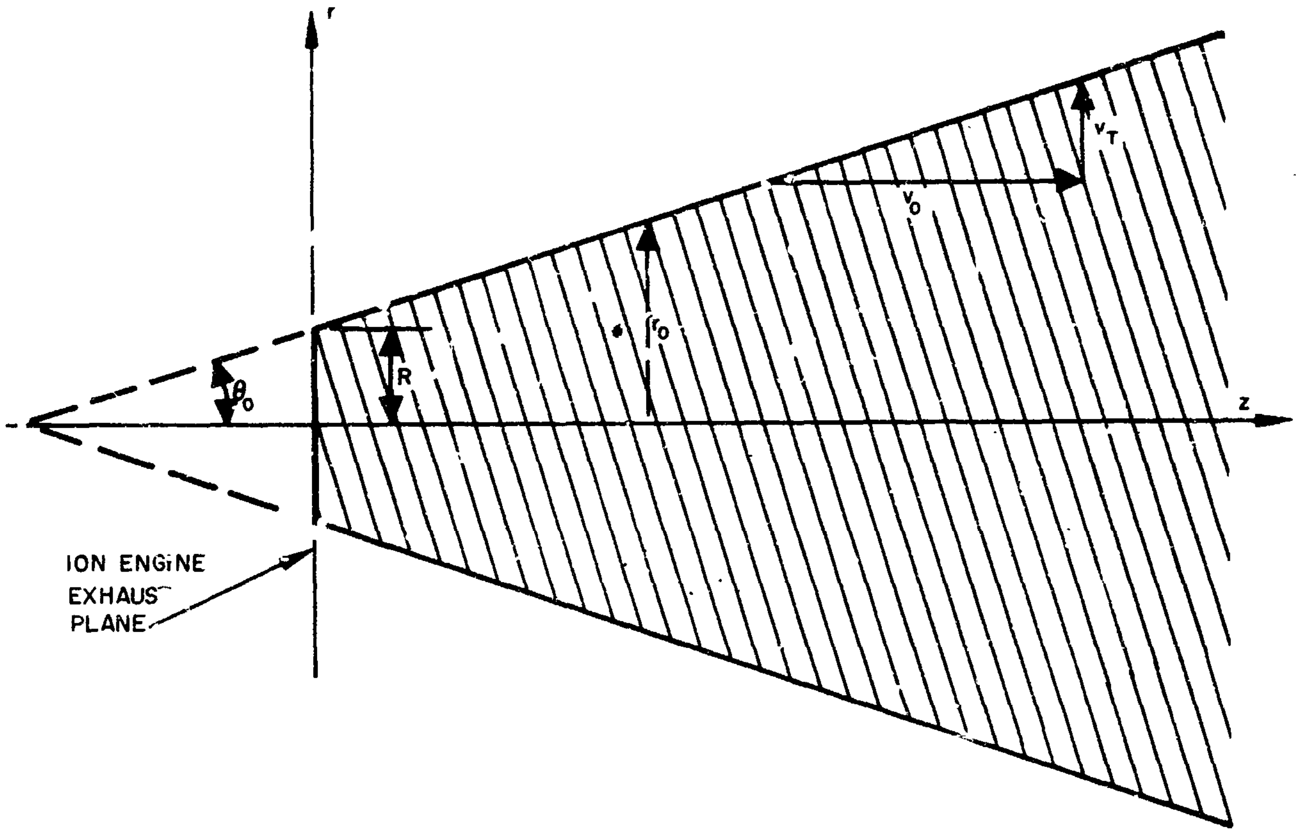

Fig. 1. Cylindrical conical wake model.

An "end" can be ascribed to the plasma when the charged particle density reaches the background density n_f. This gives

$$z_{max} = \left[\left(\frac{n_o}{n_f}\right)^{1/2} - 1\right] \frac{v_o}{v_T} R \approx \left(\frac{n_o}{n_f}\right)^{1/2} \frac{v_o}{v_T} R$$

$$r_{o\,max} = \left(\frac{n_o}{n_f}\right)^{1/2} R$$

and a persistence time for the plasma

$$\Delta t = \frac{z_{max}}{v_o} = \frac{R}{v_T}\left[\left(\frac{n_o}{n_f}\right)^{1/2} - 1\right] \approx \frac{R}{v_T}\left(\frac{n_o}{n_f}\right)^{1/2} .$$

Typical values of z_{max}, $r_{o\,max}$, and Δt are

$$z_{max} = 3.27 \times 10^6 \text{ meters}$$

$$r_{o\,max} = 1.29 \times 10^4 \text{ meters}$$

$$\Delta t = 0.268 \text{ second.}$$

All these are measured from plasma engine coordinates.

The above results apply to a plasma initially cylindrical in shape. If the plasma has an initial annular cross section, then it grows as shown in Fig. 2. After a sufficiently long time, it attains a conical outline with almost uniform density so that it approaches the model shown in Fig. 1. The density for this model is asympotically given by

$$n(z) = n_o \frac{4d}{D} \frac{1}{\left(1 + \frac{2v_T z}{v_o D}\right)^2} .$$

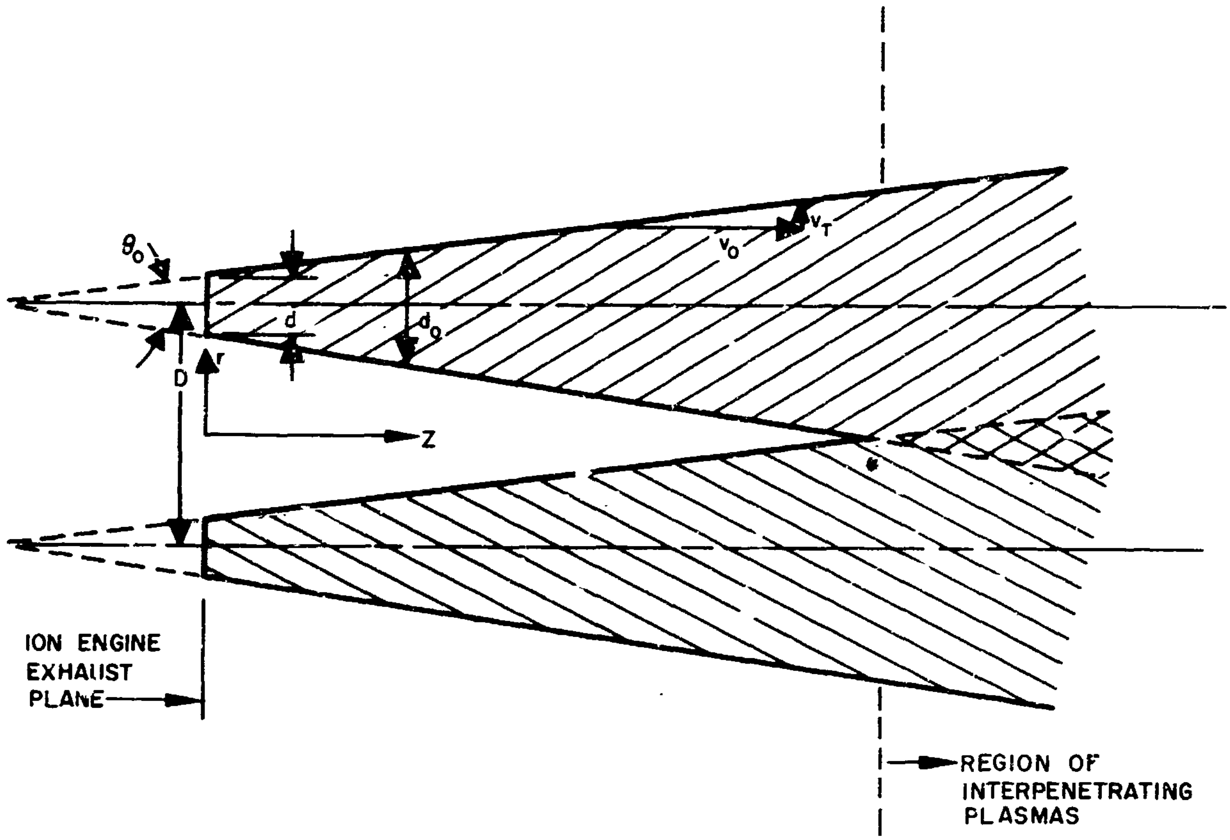

Fig. 2. Annular conical wake model.

A cluster of engines merely scales the eventual density by the number of engines.

B. MODEL FOR POWER RECEIVED BY SPACE VEHICLE ANTENNA

Noise generated in the plasma engine enters the plasma beam (exhaust, or wake), where it can freely radiate along with all the noise generated in the beam itself. An antenna aboard the space vehicle does not receive all the noise power in the beam because only a certain portion is directed toward the antenna.

If the radiation is largely caused by electrons, the distribution of radiation is nearly isotropic. This seems to be the case for the radiative processes already studied.

The plasma beam resembles a line source of radiation to an antenna on the space vehicle. According to the conical wake model, the plasma is subtended in an angle about the axis of $\theta_o = \tan^{-1} \dfrac{v_T}{v_o}$.

This is typically about 0.004 radian.

The reduction factor, defined as the power received by the antenna divided by the total power radiated, is now estimated, according to the following model.

Consider a line source, every point of which radiates isotropically. An element dz radiates an amount of power $P(z)\,dz$. A circular antenna of radius R_A lies in the x, y plane with its center at $x = y = 0$. The source extends along the axis of the antenna from $z = 0$ to $z = l$.

The power received at the antenna from an element of the source is

$$dP = \left[P(z)dz\right] \frac{\Omega(z)}{4\pi} ,$$

where

$$\Omega(z) = \int_0^{\tan^{-1}(R_A/z)} \sin\theta d\theta \int_0^{2\pi} d\phi$$

is the maximum solid angle subtended by the antenna at the element z. Solving,

$$P = \int_{o}^{\ell} \frac{P(z)}{2} \left[1 - \frac{z}{\left(R_A^2 + z^2\right)^{1/2}} \right] dz \; .$$

For the special case where the source radiates a total amount of power P_o uniformly over its length,

$$R.\,F. \equiv \text{reduction factor} = \frac{P}{P_o} = \frac{R_A}{2\ell} + \frac{1}{2}\left[1 - \left(1 + \frac{R_A^2}{2}\right)\right]^{1/2}$$

$$R.\,F. \approx \frac{R_A}{2\ell} \text{ for } \ell >> R_A \; .$$

The model can be justified for the conical wake models more rigorously, but this is not done here.

Many noise mechanisms depend on the electron density, or the ion density, but not on both. These processes radiate nearly uniformly over a certain length. Taking an antenna with a radius of 1 meter and a length corresponding to the "end" of the plasma gives a reduction factor of 1.55×10^{-7}. The reduction factor is quite significant in reducing noise at the receiving antenna.

IV. ACCOMPLISHMENTS DURING REPORT PERIOD

Several types of noise were investigated. The noise was initially calculated according to approximate models. Two types of noise were found to be significant, and these were subjected to refined calculations. These two types of noise are treated in some detail here. Only a brief summary of the other types of noise is given.

A. ELECTRON-ION COLLISIONAL RADIATION

1. Single Particle Results

The ion is assumed to be singly charged and to have infinite mass. An electron is scattered through an angle[5]

$$\theta = 2 \tan^{-1} \frac{b_o}{b} ,$$

where

$$b_o \equiv \frac{q^2}{4\pi\epsilon_o m v^2}$$

$b \equiv$ impact parameter

$q \equiv$ electron charge

$v \equiv$ asymptotic relative velocity of electron to ion

$\epsilon_o \equiv$ free space permittivity.

Only the more important long range collisions, $b \geq b_o$, are treated here.

Let the ion be located at $y = z = 0$, and let the electron come closest to the ion at time $t = 0$. The electron coordinates for long range collisions are approximately

$$y = v |t| \quad z = b \quad .$$

Only the z-component of electron motion contributes to the radiation. The z-component of electric field of the ion which acts on the electron, causing z-directed motion, is

$$E_z = \frac{q}{4\pi\epsilon_o} \frac{z}{(z^2 + y^2)^{3/2}} \approx \frac{qb}{4\pi\epsilon_o(b^2 + v^2t^2)^{3/2}} \quad .$$

The z-component of electron acceleration is

$$\ddot{z} = \dot{v}_z = -\frac{q}{m} E_z \quad .$$

Now the electric field induced by a slowly moving electron at a long distance R is

$$\vec{\mathcal{E}}(t) = \frac{q\dot{\vec{v}}(t - R/c)}{4\pi R\epsilon_o c^2} \quad .$$

Here c is the velocity of light and t - R/c accounts for the finite propagation time of the effect.

The real time variation is unimportant here; only the frequency spectrum is of interest. Taking the Fourier transform,

$$\vec{\mathcal{E}}(\omega) = \frac{1}{(2\pi)^{1/2}} \int_{-\infty}^{\infty} \vec{\mathcal{E}}(t) \quad e^{i\omega t} dt \quad ,$$

yields for the case here, ignoring a phase factor,[6]

$$\mathcal{E}_z(\omega) = \frac{1}{(2\pi)^{1/2}} \frac{q^3}{8\pi^2\epsilon_o^2 mRc^2} \frac{\omega}{v^2} K_1\left(\frac{\omega b}{v}\right) < -\infty < \omega < \infty,$$

where $K_1(x)$ is a modified Bessel function of the second kind.

The power flux in real frequency space is

$$S(\omega) = 2\epsilon_o c \; |\mathcal{E}\theta(\omega)|^2 \quad , \qquad o < \omega < \infty$$

and

$$\mathcal{E}_\theta(\omega) = -\sin\theta\ \mathcal{E}_z'(\omega) \quad .$$

The energy spectrum is

$$W(\omega) = \int_0^{2\pi}\int_0^{\pi} S(\omega)\ R^2 \sin\theta d\phi$$

while the radiated energy is

$$W = \int_0^{\infty} W(\omega)\ d\omega \quad .$$

Solving, the results for a single collision are

$$W(\omega) = \frac{q^6}{24\pi^4 \epsilon_o^3 c^3 m^2 b^2 v^2} \left[\frac{\omega b}{v} K_1\left(\frac{\omega b}{v}\right)\right]^2 \frac{\text{joules}}{\text{radian}}$$

$$W = \frac{q^6}{256\pi^2 m^2 \epsilon_o^3 c^3 b^3 v} \text{ joules} \quad .$$

2. Density Results

An electron with impact parameter in the range (b, b + db) makes dN collisions with stationary ions in one second, where

$$dN = 2\pi b db n_i v$$

and n_i is the ion particle density. Hence, the radiated power and power spectrum per electron are

$$\begin{Bmatrix} p_e(\omega) \\ p_e \end{Bmatrix} = \int_{b_{min}}^{b_{max}} \begin{Bmatrix} W_e(\omega) \\ W_e \end{Bmatrix} dN \quad .$$

Since there are n_e electrons per unit volume, the radiated spectral power density and power density are simply the above results multiplied by n_e. Also, in terms of frequency,

$$p_e(\omega)\, d\omega = p_e(2\pi f) 2\pi df \equiv p_e(f)\, df$$

so that

$$p(f) = 2\pi n_e \int_{b_{min}}^{b_{max}} W_e(2\pi f)\, dN \quad .$$

The upper limit on the integrals corresponds to a shielding distance, taken as the Debye length, h_d:

$$h_d = \left(\frac{kT\epsilon_o}{n_e q^2} \right)^{1/2} \quad \text{meters.}$$

Here, T is the electron temperature.

The lower limit corresponds to failure of the approximations used — that is, the collisions become short-range collisions involving large energy transfer. Either a classical cutoff, $b_{min} = b_o$, or a quantum mechanical cutoff $b_{min} = \frac{h}{mv}$ (h is Planck's constant) may be used. The classical distance is used here as it is larger than the quantum mechanical distance.

The integration for the power spectrum density can be done exactly; however, the result is complicated and its properties are obscure. Instead, an approximate integration is performed.

The final results are

$$p = \frac{q^6 n_i n_e}{128\pi m^2 \epsilon_o^3 c^3 b_o} = \frac{q^4 n_i n_e v^2}{32 m \epsilon_o^2 c^3} \quad \frac{\text{watts}}{m^3}$$

$$p(f) = \frac{q^6 n_i n_e}{6\pi^2 \epsilon_o^3 c^3 m^2 v} \quad g(f) \quad \frac{\text{watts}}{\text{cycle - m}^3}$$

where

$$g(f) = \begin{cases} \ln \frac{f_2}{f_1} & 0 < f < f_1 \\ \ln \frac{f_2}{f} + \frac{\pi}{4} e^{-2} - \frac{\pi}{4} e^{-2f/f_1} & f_1 < f < f_2 \\ \frac{\pi}{4} e^{-2f/f_2} & f_2 < f \end{cases}$$

$$f_1 = \frac{v}{2\pi h_d} \quad , \quad f_2 = \frac{v}{2\pi b_o} \quad .$$

The spectrum is flat out to f_1, decreases slowly out to f_2, and cuts off rapidly beyond f_2.

3. Plasma Wake Results

For the plasma wake, $n_i = n_e = n$. Using the conical wake model shown in Fig. 1,

$$n = n_o \frac{1}{\left(1 + \frac{v_T z}{v_o R}\right)^2} \quad ,$$

where πR^2 is the initial area of the (cylindrical) beam.

The results for the entire plasma are

$$\begin{Bmatrix} P \\ P(f) \end{Bmatrix} = \int_0^{2\pi} \int_0^{R\left(1+\frac{v_T z}{v_o R}\right)} \int_0^{\infty} \begin{Bmatrix} p \\ p(f) \end{Bmatrix} r dr d\phi dz \quad .$$

If the variation of n_e in the Debye length is ignored, the results are

$$P = \frac{q^4 n_o^2 v^2 v_o \pi R^3}{32 m \epsilon_o^2 c^3 v_T} = \frac{q^3 n_o v^2 R I}{32 m \epsilon_o^2 c^3 v_T} \quad \text{watts}$$

$$P(f) = \frac{q^5 n_o R I}{6\pi^2 \epsilon_o^3 c^3 m^2 v v_T} \; g(f) \; \frac{\text{watts}}{\text{cycle}} \quad ,$$

where I is the ion current.

Consideration of the variation of n_e in the Debye length introduces minor corrections in $g(f)$ which are unimportant.

4. Reduction Factor

The axial variation of noise power is

$$P(z) = \int_0^{2\pi} \int_0^{R\left(1+ \frac{v_T z}{v_o R}\right)} P \, r dr d\phi \quad .$$

The reduction factor is

$$R.F. = \frac{1}{2P} \int_0^{\infty} P(z) \left[1 - \frac{z}{\left(R_A^2 + z^2\right)^{1/2}} \; dz \right] .$$

Again, using the conical wake model of Fig. 1 and solving yields

$$R.F. \approx \frac{v_T}{v_o} \; \frac{R_A}{R} \; , \qquad \text{provided} \; \frac{v_T}{v_o} \; \frac{R_A}{R} \ll 1 \; .$$

The condition is usually true.

5. Noise Temperature

An equivalent noise temperature is defined for the plasma as the temperature at which the Johnson noise in a resistor is equal to the noise in the plasma per cycle bandwidth:

$$T_n(f) \equiv \frac{P(f)}{k} .$$

The maximum noise temperature occurs in the region $0 < f < f$ and is

$$T_n(f)_{max} = \frac{q^5 n_o I R}{6\pi^2 \epsilon_o^3 c^3 m^2 v v_T k} \ln \frac{f_2}{f_1} , \qquad {}^oK .$$

6. Quantitative Results

Using the numerical values given in Section II-D and the cylindrical conical wake model yields, for a 10-ampere cluster of engines,

total radiated noise

$$P = 2.16 \times 10^{-5} \text{ watt}$$

frequency at edge of flat portion of spectrum

$$f_1 = 1.55 \times 10^9 \text{ cps}$$

cutoff frequency

$$f_2 = 1.47 \times 10^{15} \text{ cps}$$

maximum plasma noise temperature

$$T_n = 1652\,{}^oK$$

reduction factor for receiver noise power and temperature

$$R.F. = 0.0254$$

and

$$P \times R.F. = 5.49 \times 10^{-7} \text{ watt}$$

$$T_n \times R.F. = 42\,{}^oK .$$

B. RADIATION FROM ACCELERATED ELECTRONS AT THE PLASMA BOUNDARY

The electron is reflected from the electron sheath at the boundary of the plasma and in the process of reflection radiates (noise) energy. Ions also are reflected, but their contribution to the radiation is negligible compared with that of the electrons.

1. Single Particle Results

Suppose that the interior of the plasma beam is field free and that each electron is reflected from the sheath in a time τ . Fig. 3 illustrates the process. Assume that the acceleration is constant during the time τ . The acceleration is

$$a = \frac{2v'}{\tau}$$

$$v' = \left(\frac{2}{3}\right)^{1/2} v = \left(\frac{2kT_e}{m}\right)^{1/2} .$$

Here, v' is the rms electron thermal velocity in the radial direction. The radiation formulas for a uniformly accelerated electron are well known.[6] The power radiated per collision is

$$P_e(t) = \frac{q^2 a^2}{6\pi\epsilon_o c^3} \qquad -\frac{\tau}{2} \leq t \leq \frac{\tau}{2} .$$

The energy radiated per collision is

$$W = \frac{2q^2(v')^2}{3\pi\epsilon_o c^3 \tau} .$$

The frequency spectrum of the energy is

$$W(f) = \frac{4q^2(v')^2}{3\pi\epsilon_o c^3} \left(\frac{\sin \pi f \tau}{\pi f \tau}\right)^2 \qquad \frac{\text{joules}}{\text{cycle - collision}} .$$

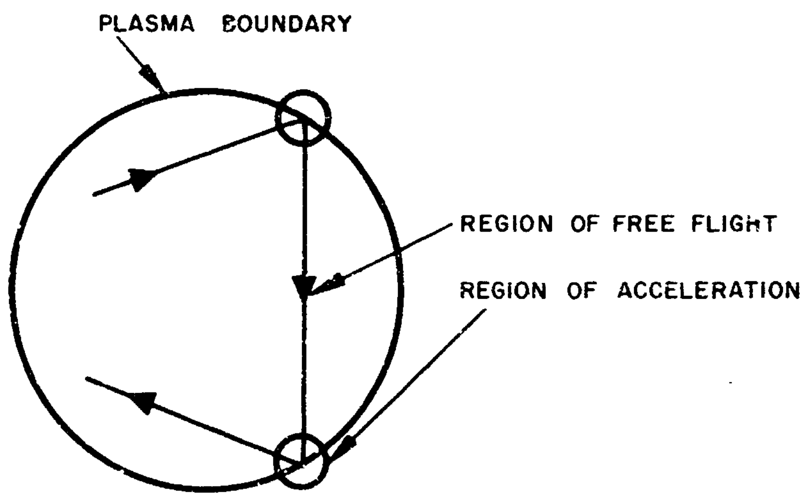

Fig. 3. Radiation at plasma boundary sheath.

The spectrum is essentially flat out to $f = 1/\tau$ and can be considered zero thereafter:

$$W(f) \approx \frac{4q^2 (v')^2}{3\pi\epsilon_o c^3} \begin{cases} 1 & f < 1/\tau \\ 0 & f > 1/\tau \end{cases} .$$

2. Density Results

Suppose d_o is the radial distance between boundary sheaths. For a cylindrical plasma, d_o is the diameter; for an annular plasma, d_o is the annular thickness. An electron of radial velocity v' makes v'/d_o collisions with a sheath in 1 second. The number of electrons per unit length, for any plasma beam cross section is

$$N_e = \frac{I}{qv_o} ,$$

where I is the ion current. The number of collisions per second per unit length is

$$N = \frac{I}{qv_o} \frac{v'}{d_o} \frac{\text{collisions}}{\text{sec - meter}} .$$

The linear power density and spectrum are now

$$P(z) = \frac{2qI(v')^3}{3\pi\epsilon_o c^3 v_o d_o \tau} \quad \frac{\text{watts}}{\text{meter}}$$

$$P(f, z) = \frac{4qI(v')^3}{3\pi\epsilon_o c^3 v_o d_o} \left(\frac{\sin \pi f\tau}{\pi f \tau}\right)^2 \quad \frac{\text{watts}}{\text{meter - cycle}}$$

$$P(f, z) \approx \frac{4qI(v')^3}{3\pi\epsilon_o c^3 v_o d_o} \begin{cases} 1 & f < 1/\tau \\ 0 & f > 1/\tau \end{cases} .$$

3. Plasma Wake Results

The radiation is dependent on the exact thickness of the plasma. Results are given for the two plasma models illustrated in Figs. 1 and 2. The variation of τ is considered as well.

a. Variation of τ — The value of τ is approximately

$$\tau = \frac{h_d}{v'} = \frac{h'_d}{v'} \left(\frac{n_o}{n}\right)^{1/2} ,$$

where h'_d is the value of h_d at the engine exhaust plane.

b. Cylindrical conical wake model (Fig. 1) — Here,

$$d_o = 2r_o = 2R\left(1 + \frac{v_T z}{v_o R}\right)$$

$$n = n_o \frac{1}{\left(1 + \frac{v_T z}{v_o R}\right)^2}$$

$$\int_o^{\infty} \frac{dz}{d_o \tau} = \frac{v_o v'}{2 v_T h'_d}$$

$$P = \frac{qI(v')^4}{3\pi\epsilon_o c^2 v_T h'_d} \quad \text{watts} .$$

The exact frequency spectrum can be obtained only in terms of tabulated integrals. However, an approximate spectrum is obtained when the approximate value of $P(f, z)$ is used. This spectrum is, where $f_1 = v'/h'_d$,

$$P(f) \approx \frac{2qI(v')^3}{3\pi\epsilon_o c^3 v_T} \ln \frac{f_1}{f} , \qquad 0 < f < f_1$$

This overestimates the results in its range. Also, it can be shown that for any f

$$P(f) \le \frac{qI(v')^3}{3\pi^3 \epsilon_o c^3 v_T} \left(\frac{f_1}{f}\right)^2 .$$

This last formula is most useful for $f > f_1$.

For $f = 0$, both formulas diverge; if z_{max} is taken to be the "end" of the plasma, rather than infinity, a finite result is obtained:

$$P(o) = \frac{qI(v')^3}{3\pi\epsilon_o c^3 v_T} \ln \frac{n_o}{n_f} .$$

c. Annular conical wake model (Fig. 2) — The outer and inner radii of the annulus varies as

$$r_2 = \frac{D + d}{2} \left[1 + \frac{2v_T z}{v_o(D + d)}\right]$$

$$r_1 = \frac{D - d}{2} \left[1 - \frac{2v_T z}{v_o(D - d)}\right] .$$

The inner radius becomes zero at

$$z_1 = \frac{v_o(D - d)}{2v_T} .$$

For $z > z_1$, the inner edges of the plasma come together, and the sheath constituting the inner boundary disappears. For $z > z_1$, assume that the plasma is uniform and obeys the conical wake model.

The radial distance between boundary sheaths is

$$d_o = \begin{cases} r_2 - r_1 & z < z_1 \\ 2r_2 & z > z_1 \end{cases} .$$

The plasma density varies as

$$n(z) = \frac{n_o}{1 + \frac{2v_T z}{v_o d}} \qquad z < z_1$$

$$n(z) = n_o \frac{4Dd}{(D+d)^2} \frac{1}{\left[1 + \frac{2v_T z}{v_o(D+d)}\right]^2} \qquad z > z_1.$$

$$\int_0^\infty \frac{dz}{d_o' \tau} = \frac{v'}{h_d'} \frac{v_o}{v_T} \left[1 - \frac{1}{2}\left(\frac{d}{D}\right)^{1/2}\right] \approx \frac{v'}{h_d'} \frac{v_o}{v_T}$$

since $d \ll D$. Hence

$$P \approx \frac{2qI(v')^4}{3\pi\epsilon_o c^3 v_T h_d'} .$$

This is twice the result of the previous model. Likewise, there is no major change in the frequency spectrum.

d. Conclusions as to models — The initial thickness of the plasma cancels out in both models and so is unimportant. The quantitative results for the two models differ by a factor of about 2, which is insignificant compared with other approximations. Either model may be used with no great error.

4. Reduction Factor

For the present case, the reduction factor is

$$R.F. = \frac{\frac{1}{2}\int_0^\infty \frac{dz}{d_o \tau}\left[1 - \frac{z}{\left(R_A^2 + z^2\right)^{1/2}}\right]}{\int_0^\infty \frac{dz}{d_o \tau}} .$$

Using the conical wake model of Fig. 1,

$$\text{R.F.} \approx \frac{v_T}{v_o} \; \frac{R_A}{R} \; , \quad \text{if} \quad \frac{v_T R_A}{v_o R} << 1 \; .$$

5. Noise Temperature

The noise temperature is defined as in Section C. The maximum noise temperature occurs for $f = 0$.

$$T_n(f)_{max} = \frac{q I (v')^3}{3\pi\epsilon_o c^3 v_T k} \left[\ln \frac{n_o}{n_f} \right] .$$

Using a more rigorous analysis, it can be shown that

$$T_n\left(\frac{f_1}{2}\right) = \frac{q I (v')^3}{3\pi\epsilon_o c^3 v_T k} \left[0.237 \right]$$

$$T_n(f_1) = \frac{q I (v')^3}{3\pi\epsilon_o c^3 v_T k} \left[0.0642 \right] .$$

6. Quantitative Results

Again, the numerical values of Section II-D are used with the cylindrical conical wake model. The results are given for a 10-ampere cluster of engines:

total radiated noise

$$P = 1.81 \times 10^{-8} \text{ watt}$$

approximate cutoff frequency

$$f_1 = 2.54 \times 10^9 \text{ cps}$$

noise temperatures

$$T_n(0) = T_{n\,max} = 3.92 \times 10^6 \ {}^oK$$

$$T_n(f_1/2) = 4.04 \times 10^4 \ {}^oK$$

$$T_n(f_1) = 1.10 \times 10^4 \ {}^oK$$

reduction factor = 0.0254

$$R.F. \times T_n(f_1) = 278 \ {}^oK .$$

C. ION-NEUTRAL BACKGROUND ATOM COLLISIONS

Ions of mass M_1 and initial velocity v_o collide head on with stationary atoms of mass M_2. The collision is assumed to be impulsive (δ function). The frequency spectrum is flat out to a cutoff frequency

$$f_1 = \frac{\Delta KE}{h} = \frac{2M_1^2 M_2 v_o^2}{h(M_1 + M_2)^2} ,$$

where ΔKE is the change in the ion's kinetic energy.

Each ion is assumed to make exactly $W/\Delta KE$ collisions, where W is the initial ion energy. The results are

$$P = \frac{2qI}{3\pi\epsilon_o c^3 h} \frac{M_1 M_2^2 v_o^4}{(M_1 + M_2)^2} \text{ watts}$$

$$P(f) = \left(\frac{qI}{3\pi\epsilon_o c^3}\right)\left(\frac{M_2 v_o^2}{M_1}\right) \frac{\text{watts}}{\text{cycle}} , \quad 0 < f < f_1$$

$$T_n(f) = \frac{P(f)}{k} .$$

As typical examples,

$$P = 5.57 \times 10^{-9} \text{ watt}$$

$$f_1 = 7.17 \times 10^{16} \text{ cps}$$

$$T_n(f) = 5.64 \times 10^{-3} \, {}^{o}K \; .$$

Also, the reduction factor is about 10^{-16}.

D. CATHODE SHOT NOISE

Electrons are assumed to be emitted randomly from the cathode. The acceleration is taken as an impulse (delta function) with the velocity after emission equal to the rms thermal velocity corresponding to the cathode temperature T_c. The energy spectrum is flat out to a maximum frequency set by quantum limitations.

The results are

$$P = \frac{3qI(kT_c)^2}{2\pi\epsilon_o c^3 mh}$$

$$f_{cutoff} = \frac{3kT_c}{2h}$$

$$P(f) = \frac{qIkT_c}{\pi\epsilon_o mc^3}$$

$$T_n(f) = \left(\frac{qI}{\pi\epsilon_o mc^3}\right) T_c \; .$$

As typical examples

$$P = 1.45 \times 10^{-9} \text{ watt}$$

$$f_{cutoff} = 3.75 \times 10^{13} \text{ cps}$$

$$T_n(f) = 2.82 \, {}^{o}K \; .$$

E. ION ACCELERATION RADIATION

In the cesium electrostatic ion engine, ions are first accelerated and then decelerated before leaving the engine. It is assumed that the electric fields are constant in each of these regions. The field is taken as the known potential change divided by the shortest length between electrode surfaces. The ion acceleration is uniform in each region. The current pulse in each acceleration region does not have a flat spectrum, but the spectrum is nearly flat out to a cutoff frequency.

Written in terms of ion acceleration and velocity change,

$$P = \frac{qI_o(\Delta v)a}{6\pi\epsilon_o c^3}$$

$$P(f) = \frac{qI_o(\Delta v)^2}{3\pi\epsilon_o c^3}\left(\frac{\sin \pi f\Delta v/a}{\pi f\Delta v/a}\right)^2$$

$$f_{\text{cutoff}} \approx \frac{a}{\Delta v} = f_1 .$$

$$T_n(f) = \frac{P(f)}{k} .$$

As typical examples, for the acceleration region

$$P = 4.12 \times 10^{-17} \text{ watt}$$

$$f_1 = 8 \times 10^6 \text{ cps}$$

$$T_{n\,max} = 0.748\ ^{\circ}\text{K} ,$$

while for the deceleration region

$$P = 2.60 \times 10^{-17} \text{ watt}$$

$$f_1 = 5.89 \times 10^7 \text{ cps}$$

$$T_{n\,max} = 0.0639\ ^{\circ}\text{K} .$$

V. PRELIMINARY CONCLUSIONS

Two important noise mechanisms have been found. These are radiation from electron-ion collisions and radiation from electron-boundary sheath collisions.

Various effects exist which reduce the noise seen by a receiver aboard the space vehicle. One major effect is that the plasma appears to radiate as a line source seen end on.

Many of the noise mechanisms studied have a frequency at which the noise per cycle bandwidth begins to decrease, either gradually or very sharply. This frequency is essentially the electron plasma frequency at the plasma engine exhaust plane.

Communication systems should probably be operated above the initial plasma frequency. In this frequency range, there is a reduction in plasma noise, and also the dielectric properties of the plasma have less effect on antenna patterns.

If a communication frequency equal to the initial plasma frequency is chosen, the maximum plasma noise temperature for that frequency thus far determined is about 11, 000°K. When the line source effect is considered, the maximum receiver noise temperature at the same frequency is about 280°K. These calculations are for a hypothetical, but possible, engine. The cesium ion engine currently under development by the Hughes Research Laboratories would have temperatures approximately 1/25 those quoted.

A noise growth mechanism may possibly exist. Further analysis is needed to ascertain this. The models of the plasma proposed here are inadequate for study of noise growth. If analysis does indicate noise growth, experimental evidence for its actual existence must be established. Only then can its importance be determined.

Unless a noise growth mechanism does exist, the noise sources already considered constitute no serious barrier to reliable communication systems.

VI. EXPERIMENTAL PLANS

No definite plans can be established until further analysis is available to guide the experiments. Any noise growth mechanism will greatly complicate experimental measurements. Some suggestions about possible experiments and some considerations on experimental complications are given here.

A. EXPERIMENTAL COMPLICATIONS

The experimental phase of the noise program is to be conducted on the (cesium) electrostatic ion engine. The test engine is mounted in a metal vacuum chamber. Because of the confined surroundings, the noise generated in this system may differ significantly from that encountered in a real space environment.

1. Cavity Effect

Radiation striking the chamber walls is not completely absorbed (proper space simulation), but is largely reflected. The radiation energy in the chamber rises to about $(\sigma/8\omega\epsilon_0)^{1/2}$ times the radiation energy in the same volume in free space. Here σ is the wall conductivity at radian frequency ω. The losses on the outer surface of the ion engine must also be incorporated into this effect. At 10^9 cps, for copper walls, the above factor is 1.14×10^4. The cavity effect gives large apparent powers in any noise measurements.

The cavity effect also destroys any directive effects of emitted radiation and leads to an isotropic, homogeneous radiation flux.

The amplitude effect of the cavity can be calibrated by using a known noise source in the chamber and measuring the power received by a detector.

2. Background Gas

Gas in space is largely hydrogen at a particle density of about $10^6/m^3$. In the vacuum chamber, the gas is initially air at about 10^{16} to 10^{14} particles/m^3. For comparison, the initial plasma beam particle density is about $10^{16}/m^3$. After prolonged ion engine operation, the neutral cesium atom level will approach the background density.

The high neutral atom density, compared with the beam density, makes diffusion effects important. This modifies the rate of expansion of the plasma beam and thus affects the generated noise level.

The high neutral atom population causes a large increase in the density of neutral atom collision radiation over that occurring in space. However, the actual total power decreases due to the short length of the plasma beam.

3. Length Effect

The noise generated due to different processes depends on the length of the plasma. In the vacuum chamber, only a short length of plasma, several meters, is available. This typically reduces the actual noise power generated by factors of 10^{-3} to 10^{-4}, compared with the noise powers given in Section IV.

4. Collector Effect

Charged particles impinging on the collector give rise to deceleration radiation. Also, secondary emission of electrons and ions occurs. These secondaries interact with the plasma beam and neutral particles to cause additional radiation. These effects are absent in space, where no collector exists.

In addition, electrons reflected or emitted from the collector contribute to and participate in any double streaming and noise growth mechanisms.

B. POSSIBLE EXPERIMENTS

1. Quantities to be Measured

Based on the conditions existing in space, the following items should be measured to test the analysis.

a. power spectrum

b. directional distribution of emitted radiation

c. variation of spectrum along the plasma beam.

The last two items require movable detectors inside the vacuum chamber. However, the cavity effect, if uncompensated, will make items b and c unmeasurable.

Essentially only the power spectrum can be measured, and the cavity effect distorts these results.

2. Frequency Range

The analysis to date indicates a flat spectrum out to the plasma frequency corresponding to the initial plasma beam particle density, about 900 Mc. Above this frequency, the spectral amplitude should decrease. The power spectrum should therefore be measured between 500 Mc and 3000 Mc.

3. Equipment Sensitivity

No detailed analysis has been made of the equipment needed. The power received by a detector mounted in the vacuum chamber is increased by the cavity effect, decreased by the short length of plasma available, and decreased somewhat more by having only one ion engine available, and not a cluster as assumed in the earlier quantitative results. It is expected that these effects nearly cancel each other.

An order of magnitude estimate indicates that receivers with noise temperatures less than 300°K are needed for spectral measurements in the 500 to 3000 Mc band.

VII. PLANS FOR NEXT QUARTER

The following items will be treated, time permitting:

1. Investigation of noise from recombination and from charge exchange processes. This seems to be the only large remaining noise source.

2. A study of the possible noise growth mechanism.

3. Initial planning of experiments to test the validity of the analytical conclusions.

REFERENCES

1. G. E. Valley, Jr., and H. Wallman, Vacuum Tube Amplifiers: Radiation Laboratory Series (McGraw-Hill Book Company, Inc., New York, 1949), Vol. 18, Chap. 12.

2. Data on ion engines correspond to actual or potential operating conditions for cesium electrostatic ion engine under development by Hughes Research Laboratories. This information was supplied by J. R. Anderson and S. Eilenberg of the Hughes Research Laboratories.

3. W. Proell and N. J. Bowman, A Handbook of Space Flight (Perstadion Press, Chicago, 1958), 2nd ed., p. 142.

4. C. Kittel, Elementary Statistical Physics (John Wiley and Sons, Inc., New York, 1958), Sec. 31, pp. 153-156.

5. L. Spitzer, Jr., Physics of Fully Ionized Gases (Interscience Publishers, Inc., New York, 1956), Chap. 5.

6. W. K. H. Panofsky and M. Phillips, Classical Electricity and Magnetism (Addison-Wesley Publishing Company, Inc., Reading, Mass., 1955), Chap. 19.